

A Low Profile Tightly Coupled Antenna Array with 80° Scanning for Multifunctional Applications

Alpha O. Bah
Global Big Data Technologies Centre
University of Technology Sydney
Sydney, Australia
alpha.bah@student.uts.edu.au

Trevor S. Bird
Global Big Data Technologies Centre
University of Technology Sydney
Sydney, Australia
trevor.bird@uts.edu.au

Peiyuan Qin
Global Big Data Technologies Centre
University of Technology Sydney
Sydney, Australia
peiyuan.qin@uts.edu.au

Abstract—A wideband wide scanning antenna array for application in multifunctional phased arrays is presented. The dipoles and balun are printed on both sides of a single RT/Duroid™ 6010 substrate with a relative dielectric constant of 10.2. Optimized designs of two thicknesses of a metasurface-based wide angle impedance matching layer are presented, facilitating the highest figure of merit values in phased array antennas. The feed network, composed of meandered impedance transformer and balun sections, are constructed from Klopfenstein tapered microstrip lines. The overall height of the array above the ground plane is $0.087 \lambda_L$, where λ_L is the wavelength at the lowest frequency of operation. For the single sided metasurface design, scanning to 80° along the E-plane and 55° along the H-plane over a 5.5:1 impedance bandwidth (0.77 GHz – 4.2 GHz) was achieved assuming an active VSWR value of 3.1.

Keywords—Antennas, tightly coupled array, Multifunctional, Metasurface, wide angle impedance matching.

I. INTRODUCTION

Low profile [1] multifunctional [2] antenna arrays over wide bandwidths have received increasing interest in recent years. One of these antennas can replace a multitude of other antennas leading to a significant reduction in weight, size, and costs. However, two main challenges remains to be overcome. Firstly, the increased scan loss due to the impedance mismatch at the aperture–air interface [3] has to be addressed appropriately. To address this problem, wide angle impedance matching (WAIM) superstrates using dielectrics [4, 5] and metasurfaces (MS) [6, 7] have been employed. The dielectric WAIMs increase the overall weight of the array and the chance of scan blindness. Current MS-WAIMs on the other hand operate over narrow bandwidths. Secondly, realizing a simple integrated balanced feed network remains a challenge. Previous attempts to solve this problem includes the use bulky feed organizers [8] and external 180° hybrids. Integrated balanced-to-unbalanced (balun) feeds [9, 10] overcame the bulk and weight limitation of the feed organizers but are usually multi-layered with complex matching networks.

This paper introduces two newly optimized arrays first introduced in [11, 12]. The arrays make use of single sided (SS) and double sided (DS) metasurface WAIMs. These optimized arrays has the highest figure of merit values compared to other similar designs in the literature. In addition, they approach the fundamental limit of arrays with constant polarisation. The MS-WAIMs are integrated with a simple wideband reactive feed network made out of

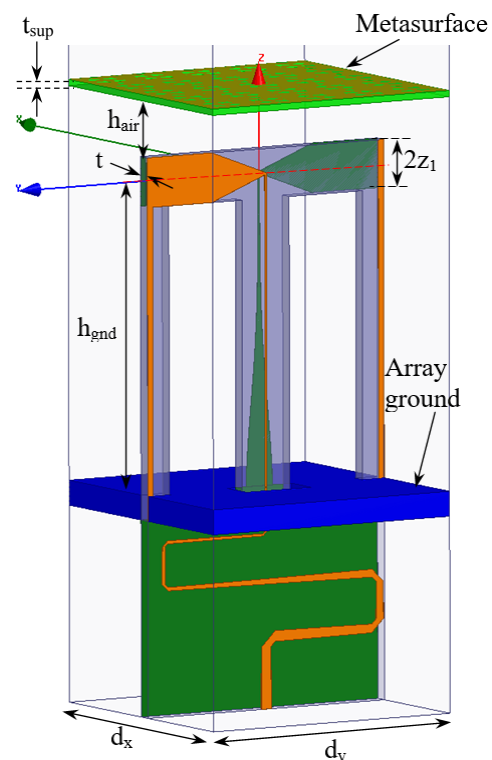


Fig. 1. Perspective view of the balun fed TCAA unit cell with a MS-WAIM superstrate. The feed and dipole was designed on a Rogers RT/Duroid™ 6010 substrate with a thickness, $t = 1.016$ mm and relative dielectric constant, $\epsilon_r = 10.2$. $d_x = d_y = 22$ mm, $z_1 = 2$ mm. $h_{gnd} = L_B + L_{add}$. Array height, $h_{array} = h_{gnd} + z_1 + h_{air} + t_{sup}$.

meandered Klopfenstein [13] tapered lines to form a tightly coupled antenna array. The optimum performing array can scan to 80° along the E-plane and 55° along the H-plane (VSWR = 3.0) over a 5.5:1 impedance bandwidth.

In this paper, the design and simulation process is reported in section II. The unit cell simulation results are presented in section III and the conclusions in section IV.

II. DESIGN AND SIMULATION

The Unit cell of the array and feed structure is depicted in Fig. 1. The dipoles and balun are printed on both sides of a single RT/Duroid™ 6010 substrate with a thickness, $t = 1.016$ mm and relative dielectric constant, $\epsilon_r = 10.2$. Using a single substrate simplifies the fabrication process. The MS-WAIM, is composed of tightly-coupled unequal arm Jerusalem cross (TC-UAJC) elements [11]. The proposed feed network consists of a meandered impedance transformer section and a

This work is supported by the Australian Government Research Training Program Scholarship, the Cooperate Research Centre for Space Environment Management (SERC Limited), and the Australia Research Council Discovery Program under Grant DE170101203 and Grant DP160102219.

balun section both of which were constructed from Klopfenstein [13] tapered microstrip lines. It converts the 50 Ω unbalanced feed to a 150 Ω balanced feed over a wide bandwidth. To provide the required wideband match, several adjustments had to be made. A length of transmission line, L_{add} , was added to the tips of the top and bottom conductors of the balun, L_B . In addition, the dimensions of the MS, the dipole, and the unit cell size were all optimized. The dipole is placed at a distance of h_{gnd} above a ground plane and covered with a MS-WAIM at a height of h_{air} . The overall height of the array above the ground plane is $0.087 \lambda_L$, where λ_L is the wavelength at the lowest frequency of operation. With the addition of the balun to the array, a common mode resonance arose around mid-band. Shorting pins were introduced to one arm of the dipole to move these resonances out of band.

The infinite array design was carried out using Floquet mode analysis and master-slave periodic boundary conditions in Ansoft HFSS [14].

III. RESULTS

Two infinite arrays were designed using a DS-MS and a SS-MS. The thickness of the DS-MS and SS-MS superstrates are 0.508 mm and 2.032 mm respectively. The detailed dimensions of the two designs and their performance parameters are given in tables I and II respectively. The DS-MS design can scan to 75° along the E-plane and 55° along the H-plane over a 5.75:1 (0.75 GHz – 4.31 GHz) broadside impedance bandwidth as shown in Fig. 2 (a). The polarization purity is > 20 dB across the band as can be seen from Fig. 2 (b). In this work, Ludwig's third definition of cross polarization is utilized [15].

TABLE I
Unit Cell Dimensions of Optimum Designs (in mm)

t_{sup}	L_{add}	h_{air}	L_B	w_{out}	y_1	y_2	y_3	r_1
0.508	2.5	4.25	22.71	0.1551	5.0	6.0	0.6	1.4
2.032	3.5	3.6	22.71	0.1551	5.0	6.0	0.5	1.4
	z_1	w_{sp}	w_s	w_{hole}	h_{hole}	t_{gnd}	d_x	d_y
0.508/2.032	2.0	0.5	2.0	6.0	3.0	2.0	22.0	22.0

TABLE II
Array Performance of Optimum Designs

t_{sup} (mm)	Array height (mm)	E-scan	H-scan	Range (GHz)	Bandwidth
0.508	31.97	75°	55°	0.75-4.31	5.75:1
2.032	33.85	80°	55°	0.77-4.20	5.46:1

*Array height = $L_B + L_{add} + h_{air} + t_{sup} + z_1$

The SS-MS design can scan to 80° along the E-plane and 55° along the H-plane over a 5.46:1 (0.77 GHz – 4.20 GHz) broadside impedance bandwidth as shown in Fig. 3 (a). The co- and cross-polarization discrimination of this design is also > 20 dB as shown in Fig. 3 (b). These designs were obtained by optimizing the array for both broadside and at the widest scan angles. The DS-MS can achieve similar performance to the SS-MS using a thinner superstrate and a lower profile array, albeit at a huge computational burden.

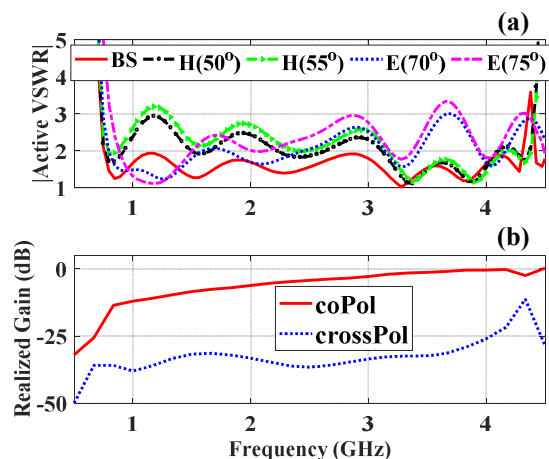


Fig. 2. The infinite dipole array performance of the DS-MS design. (a) Scanning ability (b) Co- and cross-polarized realized gains.

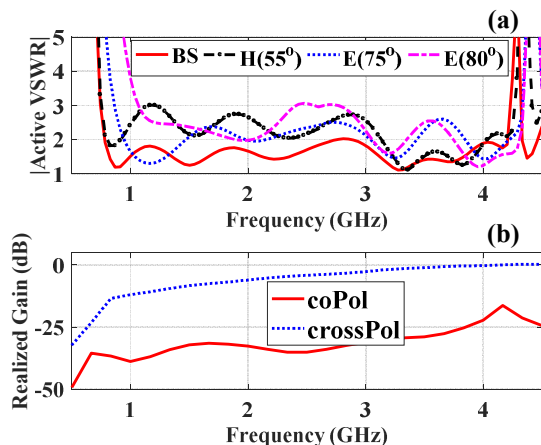


Fig. 3. The infinite dipole array performance. (a) Scanning ability. (b) Co and cross polarized realized gains.

The efficiency plot of the two designs were also obtained. The efficiency plot of the DS-MS design is displayed in Fig. 4. It has a radiation efficiency > 87 % for all scan angles across the band and a total efficiency > 80 % at broadside and > 62 % for 75° scan along the E-plane. The total efficiency for the SS-MS design is given in Fig. 5. Its radiation efficiency is > 90 % for all scan angles across the band and its total efficiency is > 80 % at broadside and > 70 % for 80° scan along the E-plane.

The array figure of merit [16], P_A , for the two arrays were also calculated using the following relation and the results displayed in Fig. 6.

$$P_A = B |\log(1 - \eta_{min})| / 2 \cos \theta_{max};$$

where $B = (\omega_{max} - \omega_{min}) / \sqrt{\omega_{max} \omega_{min}}$, θ_{max} is the maximum scan angle, \log is the natural logarithm, and η_{min} is the minimum of the total efficiency.

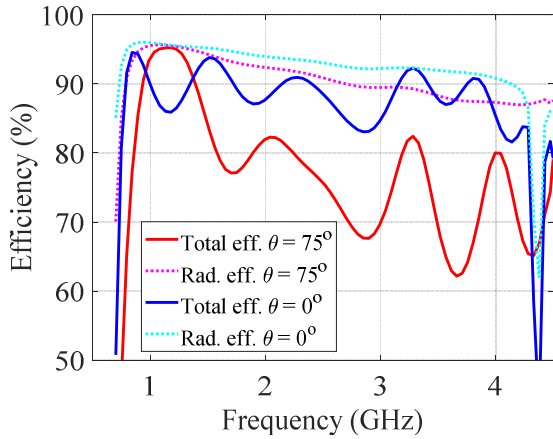


Fig. 4. Simulated total and radiation efficiencies of the DS-MS design (0.508 mm) at broadside and at 75° scan.

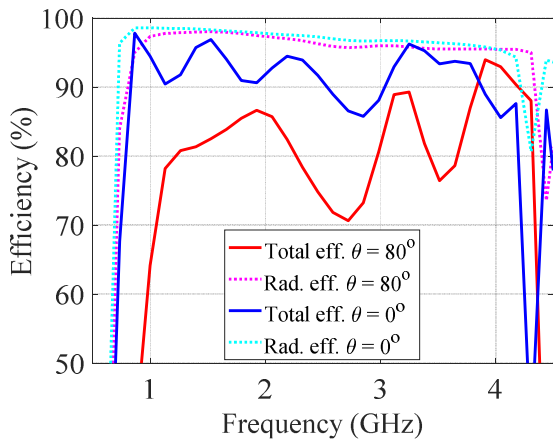


Fig. 5. Simulated total and radiation efficiencies of the SS-MS design (2.032 mm) at broadside and at 80° scan.

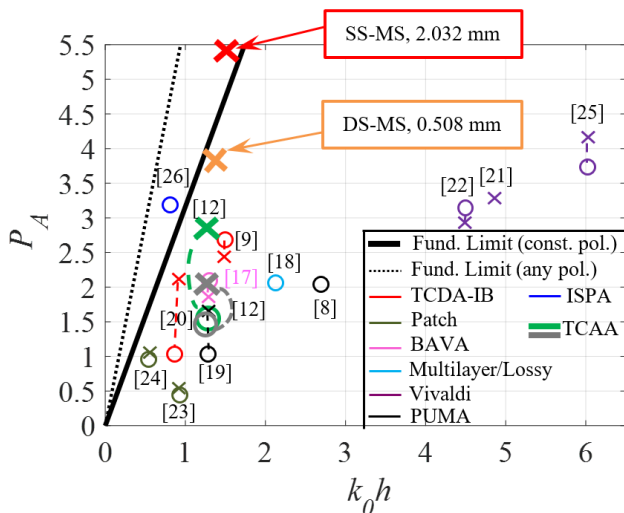


Fig. 6. Performance comparison of wideband PEC-backed antenna arrays using the array figure of merit (P_A) versus electrical thickness (k_0h) plot. This figure is reproduced here courtesy of the work done in [16] with the addition of some recently reported works. The DS-MS design and the SS-MS designs are shown in bold orange and bold red respectively. The circles represent broadside performance and the crosses represent scanning performance along the E or H planes.

The P_A of the DS-MS and SS-MS designs are shown in bold orange and bold red respectively. From Fig. 6, it can be clearly seen that the performance of the two arrays presented in this paper has the highest P_A values compared to other similar designs in the literature. In addition, they approach the fundamental limit of arrays with constant polarisation. The circles represent broadside performance and the crosses represent scanning performance along the E or H planes.

IV. CONCLUSION

A wideband wide scanning antenna array with an integrated low profile balun is presented. The overall array height is just $0.087 \lambda_L$. For the optimum SS-MS design, a bandwidth of 5.5:1 was achieved while scanning to 80° in the E-plane and 55° in the H-plane for an active VSWR value of 3.1. In addition, the fact that the balun and dipoles are printed on the same substrate, ensures simplicity in construction and cost reduction. Two designs are presented with figure of merit values approaching the fundamental limits of arrays with constant polarisation. Further improvements to the array can be achieved by increasing the array size for better radiation and matching characteristics, implementing a dual polarization setup, and using a stripline or substrate integrated waveguide (SIW) feed to reduce unwanted feed coupling. This wideband, wide scanning, array with an integrated low profile feed can serve as a multifunctional phased array for various radar, communication, and sensing applications.

ACKNOWLEDGMENT

The authors would like to thank the staff at the Faculty of Engineering and Information Technology (FEIT) workshop of the University of Technology Sydney, and the staff at Jenkins Engineering Defense Systems (JEDS) for their help with the array fabrication and measurement respectively.

REFERENCES

- [1] M. Jones and J. Rawnick, "A new approach to broadband array design using tightly coupled elements," in *Proc. IEEE MILCOM*, Oct. 2007, pp. 1-7.
- [2] G. C. Tavik, C. L. Hilterbrick, J. B. Evins, J. J. Alter, J. G. Crnkovich, J. W. De Graaf, W. Habicht, G. P. Hrin, S. A. Lessin, D. C. Wu, and S. M. Hagewood, "The advanced multifunction RF concept," *IEEE Trans. Microwave Theory Techn.*, vol. 53, no. 3, pp. 1009-1020, Mar. 2005.
- [3] A. Oliner and G. Knittel, Eds., "Phased array antennas," in *Proc. 1970 Phased Array Symposium*, 1972 (Artech House, Dedham, MA).
- [4] E. G. Magill and H. A. Wheeler, "Wide-angle impedance matching of a planar array antenna by a dielectric sheet," *IEEE Trans. Antennas Propag.*, vol. 14, no. 1, pp. 49-53, Jan. 1966.
- [5] S. Lee and R. Mittra, "Radiation from dielectric-loaded arrays of parallel-plate waveguides," *IEEE Trans. Antennas Propag.*, vol. 16, no. 5, pp. 513-519, Sep. 1968.
- [6] S. Sajuyigbe, M. Ross, P. Geren, S. A. Cummer, M. H. Tanielian, and D. R. Smith, "Wide angle impedance matching metamaterials for waveguide-fed phased-array antennas," *IET Microw. Antennas Propag.*, vol. 4, no. 8, pp. 1063-1072, Aug. 2010.
- [7] T. R. Cameron and G. V. Eleftheriades, "Analysis and characterization of a wide-angle impedance matching metasurface for dipole phased arrays," *IEEE Trans. Antennas Propag.*, vol. 63, no. 9, pp. 3928-3938, Sep. 2015.
- [8] B. Munk, R. Taylor, T. Durham, W. Crosswell, B. Pigon, R. Boozer, S. Brown, M. Jones, J. Pryor, S. Ortiz, J. Rawnick, K. Krebs, M. Vanstrum, G. Gothard, and D. Wiebelt, "A low-profile broadband phased array antenna," in *Proc. IEEE Antennas Propag. Soc. Int. Symp. (APS'03)*, Columbus, OH, USA, Jun. 2003, vol. 2, pp. 448-451.
- [9] J. P. Doane, K. Sertel, and J. L. Volakis, "A Wideband, Wide Scanning Tightly Coupled Dipole Array With Integrated Balun

- (TCDA-IB)," *IEEE Trans. Antennas Propag.*, vol. 61, no. 9, pp. 4538-4548, Sep. 2013.
- [10] J. T. Logan and M. N. Vouvakis, "On the design of 6:1 mm-wave PUMA arrays," in *Proc. Antennas and Propagation Society International Symposium (APSURSI)*, Jul. 2013, pp. 626-627.
- [11] A. O. Bah, P. Y. Qin, R. W. Ziolkowski, Q. Cheng, and Y. J. Guo, "Realization of an Ultra-thin Metasurface to Facilitate Wide Bandwidth, Wide Angle Beam Scanning," *Scientific Reports*, vol. 8, no. 1, pp. 4761, Mar. 2018.
- [12] A. O. Bah, P. Qin, R. W. Ziolkowski, Y. J. Guo, and T. S. Bird, "A Wideband Low-Profile Tightly Coupled Antenna Array With a Very High Figure of Merit," *IEEE Trans. Antennas Propag.*, vol. 67, no. 4, pp. 2332-2343, Apr. 2019.
- [13] R. W. Klopfenstein, "A Transmission Line Taper of Improved Design," *Proceedings of the IRE*, vol. 44, pp. 31-15, Jan. 1956.
- [14] ANSYS HFSS ver. 16, ANSYS, Inc., Canonsburg, PA [Online]. Available: <https://www.ansoft.com/products/hf/hfss/>
- [15] A. Ludwig, "The definition of cross polarization," *IEEE Trans. Antennas Propag.*, vol. 21, pp. 116-119, Jan. 1973.
- [16] J. P. Doane, "Wideband low-profile antenna arrays: Fundamental limits and practical implementations," Ph.D. dissertation, Dept. Elect. Comput. Eng., Ohio State Univ., Columbus, OH, USA, 2013.
- [17] M.W. Elsallal and J. C. Mather, "An ultra-thin, decade (10:1) bandwidth, modular "BAVA" array with low cross-polarization," in *Proc. IEEE Int. Symp. Antennas Propag. (APSURSI'11)*, July 2011, pp. 1980-1983.
- [18] W. F. Moulder, K. Sertel, and J. L. Volakis, "Superstrate-enhanced ultrawideband tightly coupled array with resistive FSS," *IEEE Trans. Antennas Propag.*, vol. 60, no. 9, pp. 4166-4172, 2012.
- [19] S. S. Holland and M. N. Vouvakis, "The Planar Ultrawideband Modular Antenna (PUMA) Array," *IEEE Trans. Antennas and Propag.*, vol. 60, no. 1, pp. 130-140, Jan. 2012.
- [20] E. Yetisir, N. Ghalichechian and J. L. Volakis, "Ultrawideband array with 70° scanning using FSS superstrate," *IEEE Trans. Antennas Propag.*, vol. 64, no. 10, pp. 4256-4265, Oct. 2016.
- [21] H. Holter, T.H. Chio, and D. H. Schaubert, "Experimental results of 144-element dual-polarized endfire tapered-slot phased arrays," *IEEE Trans. Antennas Propag.*, vol. 48, no. 11, pp. 1707-1718, Nov. 2000.
- [22] D. H. Schaubert, S. Kasturi, A. O. Boryszenko, and W. M. Elsallal, "Vivaldi antenna arrays for wide bandwidth and electronic scanning," in *Proc. EuCAP - European Conference on Antennas & Propagation*. IET, Nov. 2007, pp. 1-6.
- [23] M. J. Buckley, J. Wolf, B. J. Herting, J. Mather, D. Manson, and J. B. West, "Wide band and wide scan metamaterial loaded radiating elements," in *Proc. Antennas and Applications Symposium, Allerton IL*, Sep. 2010.
- [24] R. Erickson et al., "Wideband and wide scan phased array microstrip patch antennas for small platforms," in *Proc. EuCAP - European Conference on Antennas & Propagation*. IET, Nov. 2007, pp. 1-6.
- [25] M. Stasiowski and D. Schaubert, "Broadband array antenna," in *Proc. Antennas and Applications Symposium, Allerton IL*, Sep. 2008.
- [26] I. Tzanidis, K. Sertel, and J. L. Volakis, "Interwoven spiral array (ISPA) with a 10:1 bandwidth on a ground plane," *IEEE Antennas Wireless Propag. Lett.*, vol. 10, pp. 115-118, 2011.